A comparative study of averaged buck converter in mixed conduction mode with nonlinear controllers: sliding-mode and input-output linearization

Marcelo Monari Baccaro
Mechatronics engineering department
Polytechnic School of University of São Paulo
São Paulo, Brazil
marcelo.baccaro@usp.br

***Abstract*—Even in a single conduction mode, all dc-dc switching converters are nonlinear systems because theirs variable structures. There for, it's only natural to use a nonlinear control paradigm to achieve high-performance. In this paper, the state space average (SSA) dynamic model of buck converter is obtained for both conduction modes, continuous and discontinuous, as well its boundary. And two nonlinear controls architectures are studied: sliding-mode and input-output linearization (feedback linearization).**

***Index Terms*—buck converter, mixed conduction mode, sliding-mode, input-output linearization, integral action**

I. Introduction

When there is a need for wide voltage operation range, such as adjustable switch-mode power supply (ASMPS), if the load is large enough, the DC-DC converter can operate both in continuous conduction mode (CCM) or in discontinuous conduction mode (DCM), in other words, in mixed conduction mode (MCM). Therefore, it's important to obtain and study the dynamic models and controllers for both conduction modes.

The classical ideal buck converter, as shown in figure 1, has a broad application and had been studied extensively. However, the literature lacks studies comparing nonlinear controllers for MCM.

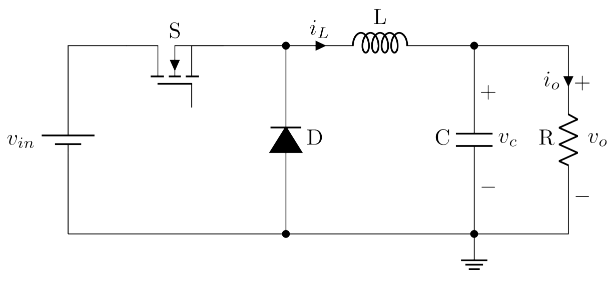

Fig. 1. Buck converter.

The exact dynamics of the buck converter is described by the piecewise linear (a kind of non-smooth with variable structure) ordinary differential equations (1) using switching functions.

$$\begin{cases} \dot{v}_C = u_2 \cdot \frac{i_L}{C} - \frac{v_C}{RC} \\ \dot{i}_L = u_2 \cdot \frac{u_1 \cdot v_{in} - v_C}{L} \end{cases} \tag{1}$$

where

$$u_1 = \begin{cases} 1, \text{ switch S is ON} \\ 0, \text{ switch S is OFF} \end{cases}$$

$$u_2 = sgn(sgn(v_L) + sgn(i_L)) = \begin{cases} 1, \text{ CCM} \\ 0, \text{ DCM} \end{cases}$$

$$v_L = u_1 \cdot v_{in} - v_C$$

$$sgn(x) = \begin{cases} 1, x > 0 \\ 0, x \leq 0 \end{cases}$$

The switching function u_2 indicates that the inductor status determines the conduction mode of the buck converter. The diode D is only ON when $sgn(v_L) = 0$ and the conduction is continuous ($u_2 = 1$), which implies $sgn(i_L) = 1$.

Although this model is exact, the only control paradigm that can be design using it is sliding mode with Δ-Σ modulation [1]. But this method has the problem of introducing high frequency excitation. To limit the operation frequency, a very common method is to use PWM (Pulse Width Modulation) with constant switching period T_s and control the modulation duty-cycle d, that only appears as the control variable in SSA models [2] and corresponds to the percentage of period when the switch S is ON. When using the PWM to regulate the output voltage $v_o \in [0, v_{in}]$ (in steady state, because it can reach $2v_{in}$ in the transient state) of the buck converter, the CCM means that the inductor never demagnetizes over the switching period and DCM means the opposite.

II. State space average (SSA) dynamic model

From equation (1), the buck converter has 3 structures, which can be put individually in the linear state space form of equation (2) with $\boldsymbol{x}^\top = [\, v_C \; i_L \,]$, $\boldsymbol{u} = v_{in}$ and $\boldsymbol{y} = v_C$.

$$\begin{cases}\dot{\boldsymbol{x}} = \boldsymbol{A}_i \cdot \boldsymbol{x} + \boldsymbol{B}_i \cdot \boldsymbol{u} \\ \boldsymbol{y} = \boldsymbol{C}_i \cdot \boldsymbol{x} + \boldsymbol{D}_i \cdot \boldsymbol{u}\end{cases} \tag{2}$$

1) CCM with switch S ON ($u_2 = 1$ and $u_1 = 1$)

$$\boldsymbol{A}_1 = \begin{bmatrix} -\frac{1}{RC} & \frac{1}{C} \\ -\frac{1}{L} & 0 \end{bmatrix} \quad \boldsymbol{B}_1 = \begin{bmatrix} 0 \\ \frac{1}{L} \end{bmatrix}$$
$$\boldsymbol{C}_1 = \begin{bmatrix} 1 & 0 \end{bmatrix} \quad \boldsymbol{D}_1 = 0$$

2) CCM with switch S OFF ($u_2 = 1$ and $u_1 = 0$)

$$\boldsymbol{A}_2 = \begin{bmatrix} -\frac{1}{RC} & \frac{1}{C} \\ -\frac{1}{L} & 0 \end{bmatrix} \quad \boldsymbol{B}_2 = \begin{bmatrix} 0 \\ 0 \end{bmatrix}$$
$$\boldsymbol{C}_2 = \begin{bmatrix} 1 & 0 \end{bmatrix} \quad \boldsymbol{D}_2 = 0$$

3) DCM ($u_2 = 0$)

$$\boldsymbol{A}_3 = \begin{bmatrix} -\frac{1}{RC} & 0 \\ 0 & 0 \end{bmatrix} \quad \boldsymbol{B}_3 = \begin{bmatrix} 0 \\ 0 \end{bmatrix}$$
$$\boldsymbol{C}_3 = \begin{bmatrix} 1 & 0 \end{bmatrix} \quad \boldsymbol{D}_3 = 0$$

A. Continuous conduction mode (CCM)

The CCM averaged dynamic model is linear and is described by equation (3) [2].

$$\begin{cases}\dot{\bar{\boldsymbol{x}}} = \boldsymbol{A}_{CCM} \cdot \bar{\boldsymbol{x}} + \boldsymbol{B}_{CCM} \cdot \boldsymbol{u} \\ \boldsymbol{y} = \boldsymbol{C}_{CCM} \cdot \bar{\boldsymbol{x}} + \boldsymbol{D}_{CCM} \cdot \boldsymbol{u}\end{cases} \tag{3}$$

where

$$\begin{aligned}
\boldsymbol{A}_{CCM} &= d \cdot \boldsymbol{A}_1 + (1-d) \cdot \boldsymbol{A}_2 = \begin{bmatrix} -\frac{1}{RC} & \frac{1}{C} \\ -\frac{1}{L} & 0 \end{bmatrix} \\
\boldsymbol{B}_{CCM} &= d \cdot \boldsymbol{B}_1 + (1-d) \cdot \boldsymbol{B}_2 = \begin{bmatrix} 0 \\ \frac{d}{L} \end{bmatrix} \\
\boldsymbol{C}_{CCM} &= d \cdot \boldsymbol{C}_1 + (1-d) \cdot \boldsymbol{C}_2 = \begin{bmatrix} 1 & 0 \end{bmatrix} \\
\boldsymbol{D}_{CCM} &= d \cdot \boldsymbol{D}_1 + (1-d) \cdot \boldsymbol{D}_2 = 0
\end{aligned}$$

The state equation of (3) can be modified to show the duty cycle as the control variable *d* resulting in the equation (4).

$$\begin{bmatrix} \dot{\bar{v}}_C \\ \dot{\bar{i}}_L \end{bmatrix} = \begin{bmatrix} -\frac{1}{RC} & \frac{1}{C} \\ -\frac{1}{L} & 0 \end{bmatrix} \cdot \begin{bmatrix} \bar{v}_C \\ \bar{i}_L \end{bmatrix} + \begin{bmatrix} 0 \\ \frac{v_{in}}{L} \end{bmatrix} \cdot d \tag{4}$$

B. Discontinuous conduction mode (DCM)

In contrast to CCM, the DCM has two periods of interest: $d_1 \cdot T_s$, witch represents the period that switch S is ON; and $d_2 \cdot T_s$, witch represents the period of demagnetization of the inductor. Then, the period when the inductor is demagnetized equals to $d_3 = T_s \cdot (1 - d_1 - d_2)$. The DCM averaged dynamic model described by equation (5) seems to be linear, but it will be shown that it actually nonlinear. It is important to take note that the SSA model for DCM must be corrected with a matrix $\boldsymbol{K}$, where the inductor current is divided by $(d_1 + d_2)$ [3].

$$\begin{cases}\dot{\bar{\boldsymbol{x}}} = \boldsymbol{A}_{DCM} \cdot \bar{\boldsymbol{x}} + \boldsymbol{B}_{DCM} \cdot \boldsymbol{u} \\ \boldsymbol{y} = \boldsymbol{C}_{DCM} \cdot \bar{\boldsymbol{x}} + \boldsymbol{D}_{DCM} \cdot \boldsymbol{u}\end{cases} \tag{5}$$

where

$$\begin{aligned}
\boldsymbol{A}_{DCM} &= (d_1 \cdot \boldsymbol{A}_1 + d_2 \cdot \boldsymbol{A}_2 + (1 - d_1 - d_2) \cdot \boldsymbol{A}_3) \cdot \boldsymbol{K} \\
&= \begin{bmatrix} -\frac{1}{RC} & \frac{1}{C} \\ -\frac{d_1+d_2}{L} & 0 \end{bmatrix} \\
\boldsymbol{B}_{DCM} &= d_1 \cdot \boldsymbol{B}_1 + d_2 \cdot \boldsymbol{B}_2 + (1 - d_1 - d_2) \cdot \boldsymbol{B}_3 = \begin{bmatrix} 0 \\ \frac{d_1}{L} \end{bmatrix} \\
\boldsymbol{C}_{DCM} &= (d_1 \cdot \boldsymbol{C}_1 + d_2 \cdot \boldsymbol{C}_2 + (1 - d_1 - d_2) \cdot \boldsymbol{C}_3) \cdot \boldsymbol{K} \\
&= \begin{bmatrix} 1 & 0 \end{bmatrix} \\
\boldsymbol{D}_{DCM} &= d_1 \cdot \boldsymbol{D}_1 + d_2 \cdot \boldsymbol{D}_2 + (1 - d_1 - d_2) \cdot \boldsymbol{D}_3 = 0 \\
\boldsymbol{K} &= \begin{bmatrix} 1 & 0 \\ 0 & \frac{1}{d_1+d_2} \end{bmatrix}
\end{aligned}$$

The state equation of (5) can be modified to show the duty cycle as the control variable d_1 resulting in the equation (6).

$$\begin{bmatrix} \dot{\bar{v}}_C \\ \dot{\bar{i}}_L \end{bmatrix} = \begin{bmatrix} -\frac{1}{RC} & \frac{1}{C} \\ -\frac{d_1+d_2}{L} & 0 \end{bmatrix} \cdot \begin{bmatrix} \bar{v}_C \\ \bar{i}_L \end{bmatrix} + \begin{bmatrix} 0 \\ \frac{v_{in}}{L} \end{bmatrix} \cdot d_1 \tag{6}$$

The variable d_2 needs to be replaced by a relation of the state variable and the buck converter parameters. For this purpose, we shall investigate the behavior of $\bar{i}_L$ in DCM as function of d_1 and d_2:

$$\bar{i}_L = \frac{I_p \cdot T_s \cdot (d_1 + d_2)}{2T_s} = \frac{I_p}{2} \cdot (d_1 + d_2) \tag{7}$$

where I_p is the peak current in DCM. A second equation must eliminate this new variable. Now, we shall investigate the behavior of v_L (isn't the averaged) in DCM as function of d_1 when the switch S in ON:

$$v_L = L \cdot \frac{di_L}{dt} = v_{in} - \bar{v}_C, \text{ for } 0 \leq t \leq d_1 T_s \tag{8}$$

Considering $\bar{v}_C$ approximately constant, equation (8) becomes:

$$\frac{I_p}{d_1 T_s} = \frac{v_{in} - \bar{v}_C}{L} \quad \Longleftrightarrow \quad I_p = d_1 \cdot T_s \cdot \frac{v_{in} - \bar{v}_C}{L} \tag{9}$$

Substituting the second equation of (9) in (7), we obtain:

$$\bar{i}_L = \frac{d_1 \cdot T_s}{2} \cdot \frac{v_{in} - \bar{v}_C}{L} \cdot (d_1 + d_2) \tag{10}$$

Rearranging to put d_2 in evidence:

$$d_2 = \frac{2L \cdot \bar{i}_L}{d_1 \cdot T_s \cdot (v_{in} - \bar{v}_C)} - d_1 \tag{11}$$

Substituting (11) in (6) and changing d_1 for d, we obtain the non-affine nonlinear averaged differential equation of DCM buck converter:

$$\begin{cases} \dot{\bar{v}}_C = \frac{\bar{i}_L}{C} - \frac{\bar{v}_C}{RC} \\ \dot{\bar{i}}_L = \frac{v_{in}}{L} \cdot d - \frac{2 \cdot \bar{v}_C \cdot \bar{i}_L}{d \cdot T_s \cdot (v_{in} - \bar{v}_C)} \end{cases} \tag{12}$$

C. Boundary conduction mode (BCM)

With two modes of conduction, there must exists a boundary between these and this is the BCM. From the literature [4], it's well known the input-output voltage gain for the buck converter in both conduction modes, even in the boundary:

1) CCM:
$$M_v = \frac{v_o}{v_{in}} = d \tag{13}$$
2) BCM:
$$M_v = \frac{v_o}{v_{in}} = d_B = 1 - \frac{2L}{T_s \cdot R} \tag{14}$$
3) DCM:
$$M_v = \frac{v_o}{v_{in}} = \frac{2}{1 + \sqrt{1 + \frac{2L}{d^2 \cdot T_s \cdot R}}} \tag{15}$$

One curious consequence of equation (14) is, if $d_B < 0 \iff R < 2L/T_s$, in another words, if the load is small enough, the buck converter only operates in CCM for any output voltage $v_o \in [0, v_{in}]$ in steady state.

To obtain a state space criteria for conduction mode discrimination, we can substitute (14) in (10) by doing $d_1 = d_B$ and $d_1 + d_2 = 1$, then the equation (16) is achieved.

$$\bar{i}_{LB} = (\frac{T_s}{2L} - \frac{1}{R}) \cdot (v_{in} - \bar{v}_C) \tag{16}$$

If $\bar{i}_L(t) > \bar{i}_{LB}(t)$, then the buck converter is in CCM. If $\bar{i}_L(t) < \bar{i}_{LB}(t)$, then it is in DCM. Else, it is in BCM.

III. Control architectures

A. Input-output linearization for DCM

The classical input-output linearization [5]–[7] supposes the state equation of the nonlinear system is affine, like (17).

$$\begin{cases} \dot{\boldsymbol{x}} = \boldsymbol{f}(\boldsymbol{x}) + \boldsymbol{g}(\boldsymbol{x}) \cdot \boldsymbol{u} \\ \boldsymbol{y} = \boldsymbol{h}(\boldsymbol{x}) \end{cases} \tag{17}$$

However, the literature of control systems provides some generalisations [8] for the input-output linearization of non-affine nonlinear systems, generally described by (18).

$$\begin{cases} \dot{\boldsymbol{x}} = \boldsymbol{f}(\boldsymbol{x}, \boldsymbol{u}) \\ \boldsymbol{y} = \boldsymbol{h}(\boldsymbol{x}) \end{cases} \tag{18}$$

Fortunately, we can use feedback linearization on equation (12). Beginning with the output $y = \bar{v}_C$, the algorithm [5] follows with the time derivation until the control variable appears.

$$\dot{y} = \dot{\bar{v}}_C = \frac{\bar{i}_L}{C} - \frac{\bar{v}_C}{RC} \tag{19}$$

$$\begin{aligned} \ddot{y} = \ddot{\bar{v}}_C &= \frac{\dot{\bar{i}}_L}{C} - \frac{\dot{\bar{v}}_C}{RC} \\ &= \frac{1}{C} \cdot (\frac{v_{in}}{L} \cdot d - \frac{2 \cdot \bar{i}_L \cdot \bar{v}_C}{d \cdot T_s \cdot (v_{in} - \bar{v}_C)} - \frac{\bar{i}_L}{RC} + \frac{\bar{v}_C}{R^2 C}) \end{aligned} \tag{20}$$

The relative order of the system is 2, then there is no internal dynamics. The goal of the input-output linearization is to replace the output natural dynamic with a equivalent control v, where we can use pole placement. Considering the exact linearization done, we would have:

$$\begin{aligned} \ddot{y} = v = \ddot{y}_d - K_1 \cdot \dot{\tilde{y}} - K_0 \cdot \tilde{y} \\ \ddot{\tilde{y}} + K_1 \cdot \dot{\tilde{y}} + K_0 \cdot \tilde{y} = 0 \end{aligned} \tag{21}$$

The variable $\tilde{y} = y - y_d$ is the tracking error and y_d is the reference to be followed. And, if $K_1, K_0 > 0$, the second equation of (21) guaranties the error $\tilde{y}$ value will converge to zero. The exact linearization can be achieved by substituting the first equation of (21) in (20), then the duty-cycle regulator d in DCM is complete:

$$C \cdot v = \frac{v_{in}}{L} \cdot d - \frac{2 \cdot \bar{i}_L \cdot \bar{v}_C}{d \cdot T_s \cdot (v_{in} - \bar{v}_C)} - \frac{\bar{i}_L}{RC} + \frac{\bar{v}_C}{R^2 C}$$

$$d^2 - \frac{L}{v_{in}} \cdot (\frac{\bar{i}_L}{RC} + C \cdot v - \frac{\bar{v}_C}{R^2 C}) \cdot d - \frac{2L \cdot \bar{i}_L \cdot \bar{v}_C}{T_s \cdot v_{in} \cdot (v_{in} - \bar{v}_C)} = 0$$

$$d^2 - 2\alpha \cdot v - \beta = 0 \quad \Longrightarrow \quad d = \alpha + \sqrt{\alpha^2 + \beta} \tag{22}$$

where

$$\alpha = \frac{L}{2v_{in}} \cdot (\frac{\bar{i}_L}{RC} + C \cdot v - \frac{\bar{v}_C}{R^2 C}) \tag{23}$$

$$\beta = \frac{2L \cdot \bar{i}_L \cdot \bar{v}_C}{T_s \cdot v_{in} \cdot (v_{in} - \bar{v}_C)} \tag{24}$$

Notice that the second equation of (22) doesn't have the negative version, because $d \in [0, 1]$ and $\beta \geq 0$ (24) in a feedback controlled buck converter.

B. Sliding-mode control (SMC) for DCM

The sliding-mode controller design starts with defining the sliding surface [5], which will be second-order:

$$s(\tilde{\boldsymbol{x}}, t) = (\frac{d}{dt} + \lambda)^{n-1} \cdot \tilde{\boldsymbol{x}} \quad \xrightarrow{n=2} \quad s(\tilde{\boldsymbol{x}}, t) = \dot{\tilde{\boldsymbol{x}}} + \lambda \cdot \tilde{\boldsymbol{x}} \tag{25}$$

Defining $\tilde{\boldsymbol{x}} = \boldsymbol{x} - \boldsymbol{x}_d$. Since the state of interest to be controlled is the capacitor voltage, then $\boldsymbol{x} = \bar{v}_C$. The parameter λ dictates the system's sliding velocity when it is captured by the sliding surface, which happens for $s(\tilde{\boldsymbol{x}}, t) = 0 \implies \dot{\tilde{\boldsymbol{x}}} + \lambda \cdot \tilde{\boldsymbol{x}} = 0$. By solving this differential equation, we will have a estimate of the value of λ for a controller that makes the system reach a percentage p of the initial tracking error within t_p seconds:

$$\begin{aligned} \tilde{\boldsymbol{x}}(t) &= \tilde{\boldsymbol{x}}(0) \cdot exp(-\lambda t) \\ \tilde{\boldsymbol{x}}(t_p) &= \tilde{\boldsymbol{x}}(0) \cdot exp(-\lambda t_p) = p \cdot \tilde{\boldsymbol{x}}(0) \\ \lambda &= \frac{ln(1/p)}{t_p}, \text{ for } 0 < p < 1 \end{aligned} \tag{26}$$

For the state space trajectory to be captured by the sliding surface, there is a criteria that is stated as a inequation [5]:

$$\frac{1}{2} \cdot \frac{d}{dt}(s^2) = s \cdot \dot{s} \leq -\eta \cdot |s| \quad \iff \quad \dot{s} \leq -\eta \cdot sign(s) \tag{27}$$

where

$$sign(x) = \begin{cases} +1, \text{ for } x > 0 \\ 0, \text{ for } x = 0 \\ -1, \text{ for } x < 0 \end{cases}$$

The term $\dot{s}$ can be derived form (25):

$$\begin{aligned} \dot{s}(\tilde{\boldsymbol{x}}, t) &= \ddot{\tilde{\boldsymbol{x}}} + \lambda \cdot \dot{\tilde{\boldsymbol{x}}} \\ &= \ddot{\boldsymbol{x}} - \ddot{\boldsymbol{x}}_d + \lambda \cdot \dot{\tilde{\boldsymbol{x}}} \\ &= F(\bar{v}_C, \bar{i}_L, d) - \ddot{\boldsymbol{x}}_d + \lambda \cdot \dot{\tilde{\boldsymbol{x}}} \end{aligned} \tag{28}$$

Substituting (28) in (27):

$$F(\bar{v}_C, \bar{i}_L, d) - \ddot{\boldsymbol{x}}_d + \lambda \cdot \dot{\tilde{\boldsymbol{x}}} \leq -\eta \cdot sign(s) \tag{29}$$

The expression of $F(\bar{v}_C, \bar{i}_L, d)$ equals the right side of (20), because $y = x = \bar{v}_C$ by definition. Considering that the parameters' values of equation (12) are known, the exact linearization done by (22) can be used to achieve $F(\bar{v}_C, \bar{i}_L, d) = v(\bar{v}_C, \bar{i}_L)$. However, in the sliding-mode paradigm, the definition (21) of v won't be the same. Instead, a new definition is proposed:

$$v = \ddot{\boldsymbol{x}}_d - \lambda \cdot \dot{\tilde{\boldsymbol{x}}} - k \cdot sign(s) = F(\bar{v}_C, \bar{i}_L, d) \tag{30}$$

Substituting (30) in (29):

$$\dot{s} = -k \cdot sign(s) \leq -\eta \cdot sign(s) \quad \iff \quad k \geq \eta \tag{31}$$

A estimate of parameter η [5] can be found by integrating the second inequation of (27) from the initial time $t_0 = 0$ to the reach time t_r, witch is the time when the state space trajectory is captured by the sliding surface, in other words, $s(\tilde{\boldsymbol{x}}, t_r) = 0$.

$$\begin{gathered} \int_0^{t_r} \dot{s} \cdot dt \leq \int_0^{t_r} -\eta \cdot sign(s) \cdot dt \\ |s(\tilde{\boldsymbol{x}}, t_r) - s(\tilde{\boldsymbol{x}}, 0)| \geq \eta \cdot (t_t - 0) \quad \iff \quad \eta \leq \frac{|s(\tilde{\boldsymbol{x}}, 0)|}{t_r} \\ \eta_{MAX} = \frac{|s(\tilde{\boldsymbol{x}}, 0)|}{t_r} = \frac{|\dot{\tilde{\boldsymbol{x}}}(0) + \lambda \cdot \tilde{\boldsymbol{x}}(0)|}{t_r} \\ \eta_{MAX} = \frac{|\dot{\boldsymbol{x}}(0) - \dot{\boldsymbol{x}}_d(0) + \lambda \cdot (\boldsymbol{x}(0) - \boldsymbol{x}_d(0))|}{t_r} \end{gathered}$$

For a servomechanism tracking problem, we have $\dot{\boldsymbol{x}}_d = 0$ and $\boldsymbol{x}_d = v_r$, witch is a DC level voltage. And considering that the system begins at a steady state point, that is $\dot{\boldsymbol{x}}(t_{SS}) = 0$ and $\boldsymbol{x}(t_{SS}) = x_{SS}$. Notice that maximum displacement error is $\tilde{\boldsymbol{x}}_{MAX} = |v_r - x_{SS}|_{MAX} = v_{in}$, because $\bar{v}_C \in [0, v_{in}]$ for a voltage mode controlled buck converter. Then, the expression of η_{MAX} can be refined and substituted in (31):

$$\eta_{MAX} = \frac{\lambda \cdot v_{in}}{t_r} \quad \implies \quad k \geq \frac{\lambda \cdot v_{in}}{t_r} \tag{32}$$

Until now, we deduced the minimum controller gain k considering the parameters of $F(\bar{v}_C, \bar{i}_L, d)$ are known, so the exact linearization (22) can be done. But that's not the case when a parameter mismatch occurs. Before investigating this case, we need to define some parts of $F(\bar{v}_C, \bar{i}_L, d)$, witch is define by the right side of (20):

$$F(\bar{v}_C, \bar{i}_L, d) = f(\bar{v}_C, \bar{i}_L) + g_1(\bar{v}_C, \bar{i}_L) \cdot d + \frac{g_2(\bar{v}_C, \bar{i}_L)}{d} \tag{33}$$

where

$$\begin{aligned} f(\bar{v}_C, \bar{i}_L) &= \frac{\bar{v}_C}{(RC)^2} - \frac{\bar{i}_L}{RC^2} \\ g_1(\bar{v}_C, \bar{i}_L) &= \frac{v_{in}}{LC} \\ g_2(\bar{v}_C, \bar{i}_L) &= -\frac{2 \cdot \bar{i}_L \cdot \bar{v}_C}{d \cdot T_s \cdot (v_{in} - \bar{v}_C)} \end{aligned}$$

In a scenario where a mismatch occurs for every parameter of F, the buck converter parameters are R, L, C, v_{in} and T_S, in contrast with the controller assumed parameters, that are $\hat{R}$, $\hat{L}$, $\hat{C}$, $\hat{v}_{in}$ and $\hat{T}_s$. Then, the tentative input-output linearization is $\hat{d} = \hat{\alpha} + \sqrt{\hat{\alpha}^2 + \hat{\beta}}$. Resulting in a very different inequation from (31) when (27) is analysed:

$$\begin{aligned} \dot{s}(\tilde{\boldsymbol{x}}, t) = F(\bar{v}_C, \bar{i}_L, \hat{d}) - \ddot{\boldsymbol{x}}_d + \lambda \cdot \dot{\tilde{\boldsymbol{x}}} \leq -\eta \cdot sign(s) \\ f + g_1 \cdot \hat{d} + \frac{g_2}{\hat{d}} - \ddot{\boldsymbol{x}}_d + \lambda \cdot \dot{\tilde{\boldsymbol{x}}} \leq -\eta \cdot sign(s) \end{aligned} \tag{34}$$

This problem isn't trivial to solve. Fortunately, the analytical solution can be worked around by setting k with a high value and simulating the controller for model validation. Although the sliding-mode controller defined by (22), (25) and (30) can be robust and make the voltage output $\bar{v}_C$ converge to a DC level, the steady state error won't be zero. A sliding-mode controller with integral action can make it zero.

C. Sliding-mode control with integral action for DCM

With the integral action, the sliding surface differs from (25) and is now third-order:

$$\begin{gathered} s(\tilde{\boldsymbol{x}},t) = (\frac{d}{dt}+\lambda)^{n-1}\cdot\int_0^t \tilde{\boldsymbol{x}}\cdot\, d\tau \quad \xrightarrow{n=3} \\ s(\tilde{\boldsymbol{x}},t) = \dot{\tilde{\boldsymbol{x}}} + 2\lambda\cdot\tilde{\boldsymbol{x}} + \lambda^2\cdot\int_0^t \tilde{\boldsymbol{x}}\cdot\, d\tau \end{gathered} \tag{35}$$

As well its time derivative differs form (28):

$$\begin{aligned} \dot{s}(\tilde{\boldsymbol{x}},t) &= \ddot{\tilde{\boldsymbol{x}}} + 2\lambda\cdot\dot{\tilde{\boldsymbol{x}}} + \lambda^2\cdot\tilde{\boldsymbol{x}} \\ &= \ddot{\boldsymbol{x}} - \ddot{\boldsymbol{x}}_d + 2\lambda\cdot\dot{\tilde{\boldsymbol{x}}} + \lambda^2\cdot\tilde{\boldsymbol{x}} \\ &= F(\bar{v}_C,\bar{i}_L,d) - \ddot{\boldsymbol{x}}_d + 2\lambda\cdot\dot{\tilde{\boldsymbol{x}}} + \lambda^2\cdot\tilde{\boldsymbol{x}} \end{aligned} \tag{36}$$

Substituting (36) in (27):

$$F(\bar{v}_C,\bar{i}_L,d) - \ddot{\boldsymbol{x}}_d + 2\lambda\cdot\dot{\tilde{\boldsymbol{x}}} + \lambda^2\cdot\tilde{\boldsymbol{x}} \le -\eta\cdot sign(s) \tag{37}$$

Again, considering that the parameters' values of equation (12) are known, the exact linearization done by (22) can be used to achieve $F(\bar{v}_C,\bar{i}_L,d) = v(\bar{v}_C,\bar{i}_L)$. But v is now defined as:

$$v = \ddot{\boldsymbol{x}}_d - 2\lambda\cdot\dot{\tilde{\boldsymbol{x}}} - \lambda^2\cdot\tilde{\boldsymbol{x}} - k\cdot sign(s) = F(\bar{v}_C,\bar{i}_L,d) \tag{38}$$

Composing (38) and (37) with (27), the same result as stated in (31), $k \ge \eta$, is achieved. Although, η_{MAX} has the same expression as stated in (32), the expression for λ differs from (26):

$$\begin{gathered} s(\tilde{\boldsymbol{x}},t) = \dot{\tilde{\boldsymbol{x}}} + 2\lambda\cdot\tilde{\boldsymbol{x}} + \lambda^2\cdot\int_0^t \tilde{\boldsymbol{x}}\cdot\, d\tau = 0 \\ \ddot{\tilde{\boldsymbol{x}}} + 2\lambda\cdot\dot{\tilde{\boldsymbol{x}}} + \lambda^2\cdot\tilde{\boldsymbol{x}} = 0 \\ \tilde{\boldsymbol{x}}(t) = \tilde{\boldsymbol{x}}(0)\cdot exp(-\lambda t)\cdot(1+\lambda t) \\ \tilde{\boldsymbol{x}}(t_p) = \tilde{\boldsymbol{x}}(0)\cdot exp(-\lambda t_p)\cdot(1+\lambda t_p) = p\cdot\tilde{\boldsymbol{x}}(0) \\ exp(-\lambda t_p)\cdot(1+\lambda t_p) - p = 0 \end{gathered} \tag{39}$$

This last equation is a transcendental one, thus it can only be solved numerically. As in (34), the mismatched parameters sliding surface attraction criteria isn't trivial to solve:

$$f + g_1\cdot\hat{d} + \frac{g_2}{\hat{d}} - \ddot{\boldsymbol{x}}_d + 2\lambda\cdot\dot{\tilde{\boldsymbol{x}}} + \lambda^2\cdot\tilde{\boldsymbol{x}} \le -\eta\cdot sign(s) \tag{40}$$

The sliding-mode controller with integral action is defined by (22), (35) and (38). It's more robust that the sliding-mode controller of the previous subsection, because it can endure constant parameters mismatches or slow varying ones and guaranties zero steady state error.

A import characteristic of the sliding-mode equivalent control v of (30) and (38) is use of the function $sign(s)$ (signal of s). Although it can make the controllers work, the phenomenon of *chattering* may be present, making state space trajectory bounce over the sliding surface, which may rise the output voltage ripple. To mitigate its affect, it's common to replace the $sign(s)$ function by $sat(s/\phi)$ (saturation of s/ϕ), defined as:

$$sat(x) = \begin{cases} +1, \text{ for } x \ge 1 \\ x, \text{ for } -1 < x < 1 \\ -1, \text{ for } x \le 1 \end{cases}$$

The parameter ϕ is defined as [5]:

$$\phi = \tilde{\boldsymbol{x}}_f\cdot\lambda^{n-1} \tag{41}$$

where n is the sliding-mode controller order and $\tilde{\boldsymbol{x}}_f$ is the allowed steady state error.

D. Linear control for CCM

The linear controller for CCM (4) can be designed with state augmented integral action [9]. But the transition between CCM and DCM won't be smooth. Therefore, the input-output linearization is preferable, like (19) and (20):

$$\dot{y} = \dot{\bar{v}}_C = \frac{\bar{i}_L}{C} - \frac{\bar{v}_C}{RC} \tag{42}$$

$$\begin{aligned} \ddot{y} = \ddot{\bar{v}}_C &= \frac{\dot{\bar{i}}_L}{C} - \frac{\dot{\bar{v}}_C}{RC} \\ &= \frac{1}{C}\cdot(\frac{v_{in}}{L}\cdot d - \frac{\bar{v}_C}{L} - \frac{\bar{i}_L}{RC} + \frac{\bar{v}_C}{R^2C}) \\ &= G(\bar{v}_C,\bar{i}_L,d) \end{aligned} \tag{43}$$

Doing $G(\bar{v}_C,\bar{i}_L,d) = v(\bar{v}_C,\bar{i}_L)$, we have:

$$\begin{gathered} \frac{v_{in}}{L}\cdot d - \frac{\bar{v}_C}{L} - \frac{\bar{i}_L}{RC} + \frac{\bar{v}_C}{R^2C} = C\cdot d \\ d = \frac{1}{v_{in}}\cdot(L\cdot(C\cdot v + \frac{1}{RC}\cdot(\bar{i}_L - \frac{\bar{v}_C}{R})) + \bar{v}_C) \end{gathered} \tag{44}$$

The equivalent control v can assume the structure of (21), (30) and (38).

E. State observer

The most basic state observer is the Luenberguer observer, which comes in two versions [9], [10]:

1) Linear:

$$\dot{\hat{\boldsymbol{x}}} = \boldsymbol{A} \cdot \hat{\boldsymbol{x}} + \boldsymbol{B} \cdot d + \boldsymbol{L} \cdot (\boldsymbol{y} - \boldsymbol{C} \cdot \hat{\boldsymbol{x}}) \tag{45}$$

2) Nonlinear:

$$\dot{\hat{\boldsymbol{x}}} = f(\hat{\boldsymbol{x}}, d) + \boldsymbol{L} \cdot (\boldsymbol{y} - \boldsymbol{C} \cdot \hat{\boldsymbol{x}}) \tag{46}$$

For the linear case, the pole placement technique is used to calculate the observer gain L that imposes the eigenvalues of $(\boldsymbol{A}^\top - \boldsymbol{L}^\top \cdot \boldsymbol{C}^\top)$. And, for the nonlinear case, the procedure is more complex [10], but it follows the same reasoning. Unfortunately, this kind of observer isn't robust, but it works very well without parameters mismatches or noise.

IV. Simulations and Results

All simulations were done in the Matlab/Simulink©2015b platform. The nominal parameters of ideal buck converter are: $R = 100\Omega$, $L = 100\mu H$, $C = 50\mu F$, $v_{in} = 30V$ and $T_s = 10\mu s$. The control objective is reach the desired voltage output within 0.2s, considering as input reference the sequence [2, 26, 14] that oscillates with a period of 0.2s. The pole placement controller gains are $K_1 = 2.5743e3$ and $K_0 = 1.1505e6$. The observer gain is $L^\top = 1e3 \cdot [7.7945, -6.8044]$. And the sliding-mode controller gains are $\lambda = 700$ and $k = \lambda \cdot v_{in}/0.1 = 2.625e6$, however the sliding-mode with integral action controller of subsection IV-D uses the gain $k_{IA} = 100 \cdot k = 2.625e8$.

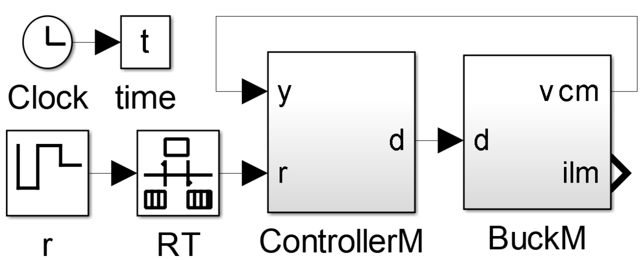

Fig. 2. Simulink block diagram of the feedback control system.

The figures 2, 3 and 4 show the Simulink block diagrams used in the simulations of the controllers of subsections IV-A to IV-D, however the last one uses a different controller block diagram. The Matlab code of the buck SSA model is presented at listing 1.

Listing 1. Code of buck SSA model

```
function [dvc, dil, mp] = fcn(d, vc, il,
    Vim, Rm, Lm, Cpm, Ts, DBm)
dvc = (il − vcRm) Cpm;
ilb = DBm (Vim − vc);
if il ilb % Nonlinear
```

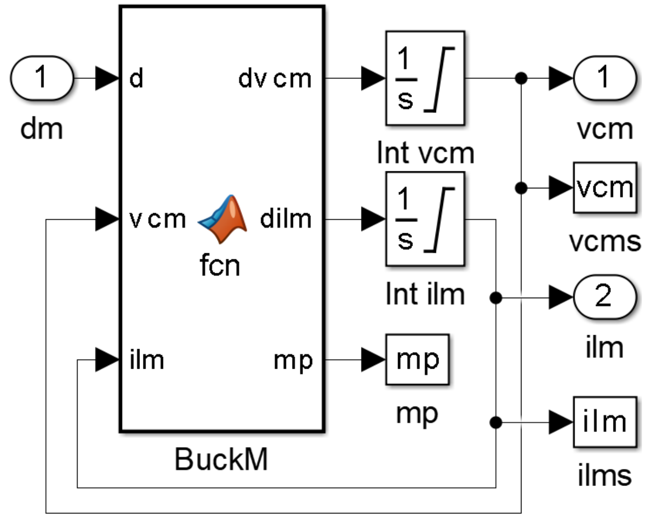

Fig. 3. Simulink block diagram of the SSA model of buck converter.

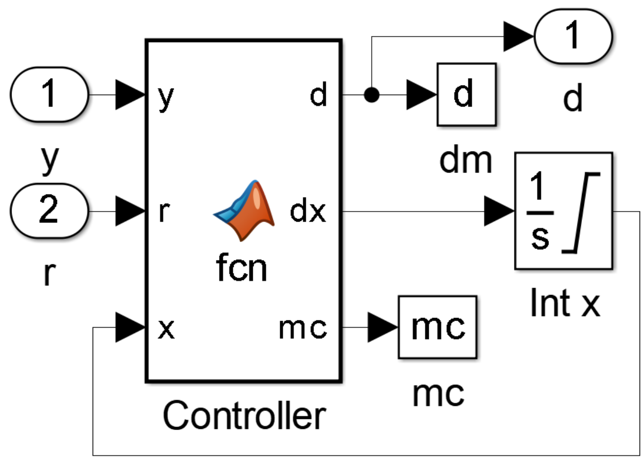

Fig. 4. Simulink block diagram of the SSA controller.

```
    dil = VimdLm − 2ilvc(dTs(Vim−vc));
    mp = 0;
else % Linear
    dil = VimdLm − vcLm;
    mp = 1;
end
```

A. Input-output linearization with pure pole placement controller (PPC) with observer

The controller code inside the block *Controller* of figure 4, presented at listing 2, uses the exact linearization (22) and (44) for, respectively, DCM (nonlinear) and CCM (linear) with pole placement in the equivalent control (21). The observer has the structure (45) for the CCM, and (46) for DCM. The simulation results are shown at figures 5 and 6.

Listing 2. Code of PPC

```
function [d, dx, mc] = fcn(y, r, x, K1,
    K0, R, Cp, L, Vi, Ts, DBm, A, B, C,
    L_fpe)
```

```
vcm = x(1);
ilm = x(2);
ilb = DBm * (Vi - vcm); % Boundary
if ilm < ilb %%% NONLINEAR %%%
    % Controller
    v = - K1 * (ilm - vcm/R) / Cp - K0 * (vcm - r);
    a = L * ((ilm - vcm/R)/(R*Cp) + Cp*v) / (2*Vi);
    b = 2 * ilm * vcm * L / (Vi * Ts * abs(Vi - vcm));
    d = a + sqrt(a^2 + b);
    % Observer
    xs1 = (ilm - vcm/R) / Cp;
    xs2 = Vi*d/L - 2*ilm*vcm/(d*Ts*(Vi-vcm));
    dx = [xs1; xs2] + L_fpe * (y - C*x);
    mc = 0;
else %%% LINEAR %%%
    % Controller
    v = - K1 * (ilm - vcm/R) / Cp - K0 * (vcm - r);
    d = (L * (Cp*v + (ilm - vcm/R) / (R*Cp)) + vcm) / Vi;
    % Observer
    dx = A*x + B*d + L_fpe * (y - C*x);
    mc = 1;
end

if d > 1
    d = 1;
elseif d < 1e-10
    d = 1e-10;
end
```

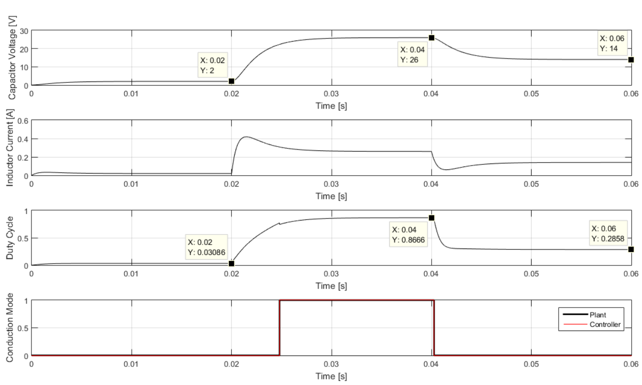

Fig. 5. Buck simulation output.

B. Input-output linearization with mixed pole placement and sliding-mode controller with observer

The controller code inside the block *Controller* of figure 4, presented at listing 3, uses the exact linearization (22) and (44) for, respectively, DCM (nonlinear) and CCM (linear), but pole

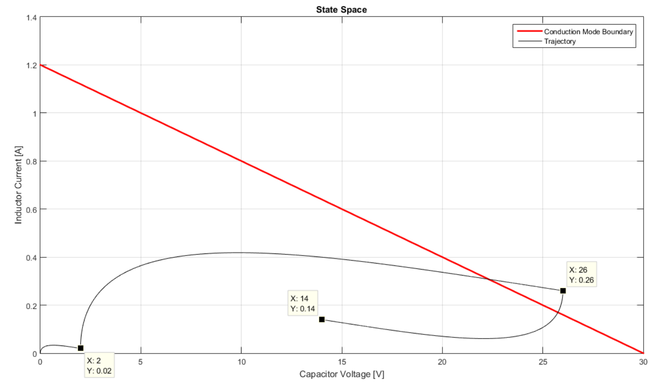

Fig. 6. Buck simulation output in state space.

placement (21) is used for the linear part and sliding-mode (30) is used for the nonlinear part as the equivalent control. The observer has the structure (45) for the CCM, and (46) for DCM. The simulation results are shown at figures 7 and 8.

Listing 3. Code of mixed PPC and SMC

```
function [d, dx, mc] = fcn(y, r, x, R, Cp, L, Vi, Ts, DBm, lambda, phi, Ks, A, B, C, L_fpe, K0, K1)
vcm = x(1);
ilm = x(2);
ilb = DBm * (Vi - vcm); % Boundary
dvcm = (ilm - vcm/R) / Cp;
if ilm < ilb %%% NONLINEAR %%%
    % Controller
    s = dvcm + lambda * (vcm - r);
    sat_s = min(1, max(-1, s/phi));
    v = - lambda * dvcm - Ks * sat_s;
    a = L * (ilm/(R*Cp) - vcm/(R^2*Cp) + Cp*v) / (2*Vi);
    b = 2 * ilm * vcm * L / (Vi * Ts * (Vi - vcm));
    d = a + sqrt(a^2 + b);
    % Observer
    xs1 = dvcm;
    xs2 = Vi*d/L - 2*ilm*vcm/(d*Ts*(Vi-vcm));
    dx = [xs1; xs2] + L_fpe * (y - C*x);
    mc = 0;
else %%% LINEAR %%%
    % Controller
    v = - K1 * dvcm - K0 * (vcm - r);
    d = (L * (Cp*v + (ilm - vcm/R) / (R*Cp)) + vcm) / Vi;
    % Observer
    dx = A*x + B*d + L_fpe * (y - C*x);
    mc = 1;
end

if d > 1
    d = 1;
```

```
elseif d < 1e-10
    d = 1e-10;
end
```

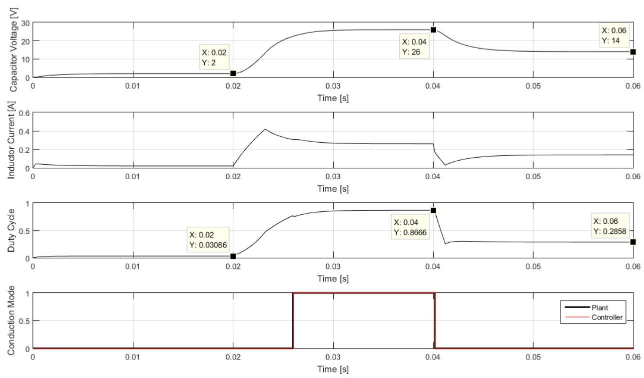

Fig. 7. Buck simulation output.

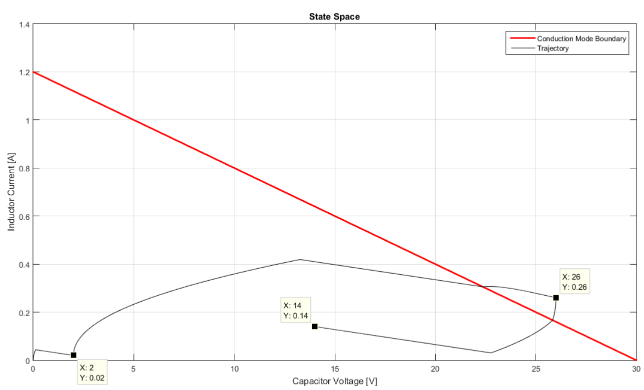

Fig. 8. Buck simulation output in state space.

C. Input-output linearization with pure sliding-mode controller (SMC) with observer

The controller code inside the block *Controller* of figure 4, presented at listing 4, uses the exact linearization (22) and (44) for, respectively, DCM (nonlinear) and CCM (linear) with sliding-mode in the equivalent control (30). The observer has the structure (45) for the CCM, and (46) for DCM. The simulation results are shown at figures 9 and 10.

Listing 4. Code of SMC

```
function [d, dx, mc] = fcn(y, r, x, R, Cp
    , L, Vi, Ts, DBm, lambda, phi, Ks, A,
    B, C, L_fpe)
vcm = x(1);
ilm = x(2);
ilb = DBm * (Vi - vcm); % Conduction Mode
    Boundary
dvcm = (ilm - vcm/R) / Cp;
% Sliding Surface
s = dvcm + lambda * (vcm - r);
% Slinding-Mode Controller
sat_s = min(1, max(-1, s/phi));
v = - lambda * dvcm - Ks * sat_s;
if ilm < ilb %%% NONLINEAR %%%
    % Controller - Input-Output
        Linearization
    a = L * (ilm/(R*Cp) - vcm/(R^2*Cp) +
        Cp*v) / (2*Vi);
    b = 2 * ilm * vcm * L / (Vi * Ts * (
        Vi - vcm));
    d = a + sqrt(a^2 + b);
    % Observer - Nonlinear Luenberguer
    dx = [dvcm; Vi*d/L-2*ilm*vcm/(d*Ts*(
        Vi-vcm))] + L_fpe * (y - C*x);
    mc = 0;
else              %%% LINEAR        %%%
    % Controller - Pole Placement with
        Tracking
    d = (L * (Cp*v + (ilm - vcm/R) / (R*
        Cp)) + vcm) / Vi;
    % Observer - Linear Luenberguer
    dx = A*x + B*d + L_fpe * (y - C*x);
    mc = 1;
end

if d > 1
    d = 1;
elseif d < 1e-10
    d = 1e-10;
end
```

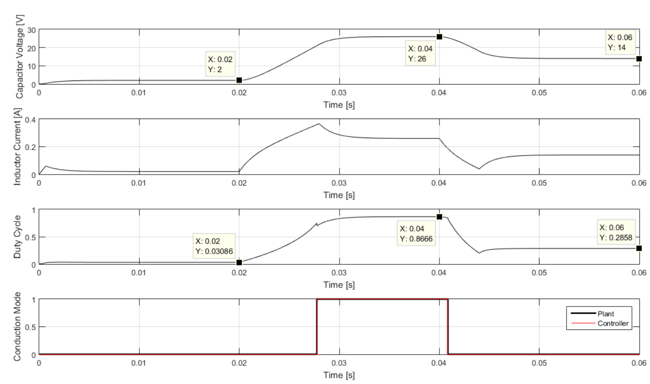

Fig. 9. Buck simulation output.

D. Input-output linearization with pure sliding-mode with integral action controller (SMIAC) without observer

The controller code inside the block *Controller* of figure 11, presented at listing 4, uses the exact linearization (22) and (44) for, respectively, DCM (nonlinear) and CCM (linear) with sliding-mode with integral action in the equivalent control (38). There is no observer because the structures (45) and (46) aren't robust, thus the parameters mismatches ruins the convergence. For the buck converter with the same nominal parameters, the simulation results are shown at figures 12 and

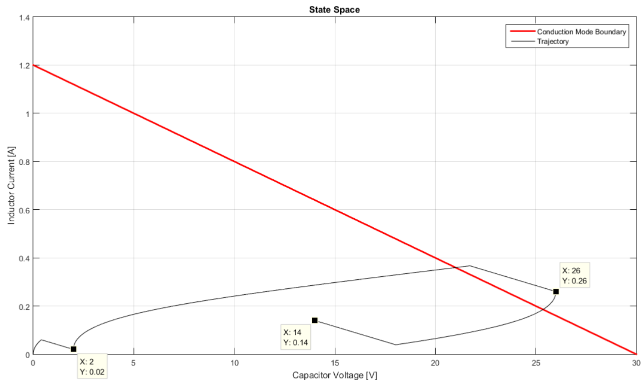

Fig. 10. Buck simulation output in state space.

13. For the buck converter with decreased parameters, where $R_m = 0.9 \cdot R$, $L_m = 0.9 \cdot L$, $C_m = 0.9 \cdot C$ and $v_{inm} = 0.98 \cdot v_{in}$, the simulation results are shown at figures 14 and 15. For the buck converter with increased parameters, where $R_m = 1.1 \cdot R$, $L_m = 1.1 \cdot L$, $C_m = 1.1 \cdot C$ and $v_{inm} = 1.02 \cdot v_{in}$, the simulation results are shown at figures 16 and 17.

Listing 5. Code of SMIAC

```
function [d, mc, dw] = fcn(vcm, ilm, r, w, R, Cp, L, Vi, Ts, DBm, lambda, phi, Ks)
ilb = DBm * (Vi - vcm); % Conduction Mode Boundary
dvcm = (ilm - vcm/R) / Cp;
dw = vcm - r;
% Sliding Surface
s = dvcm + 2 * lambda * dw + lambda^2 * w;
% Slinding-Mode Integral Action Controller
sat_s = min(1, max(-1, s/phi));
v = - 2 * lambda * dvcm - lambda^2 * dw - Ks * sat_s;
if ilm < ilb %%%   NONLINEAR   %%%
    % Controller - Input-Output Linearization
    a = L * ((ilm - vcm/R)/(R*Cp) + Cp*v) / (2*Vi);
    b = 2 * ilm * vcm * L / (Vi * Ts * (Vi - vcm));
    d = a + sqrt(a^2 + b);
    mc = 0;
else         %%%   LINEAR      %%%
    % Controller - Pole Placement with Tracking
    d = (L * (Cp*v + (ilm - vcm/R) / (R*Cp)) + vcm) / Vi;
    mc = 1;
end

if d > 1
    d = 1;
elseif d < 1e-10
    d = 1e-10;
end
```

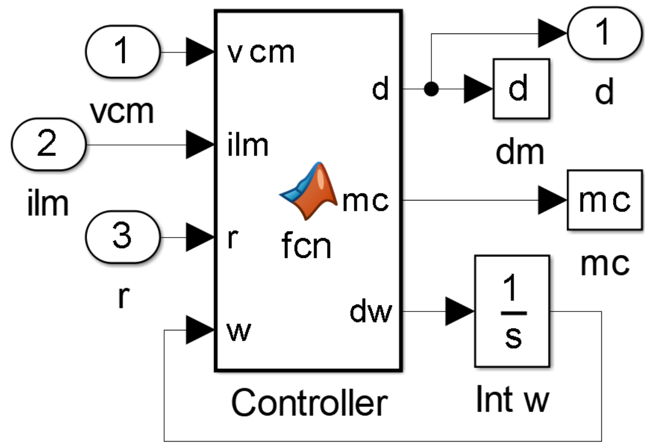

Fig. 11. Simulink block diagram of the SSA SMIAC controller.

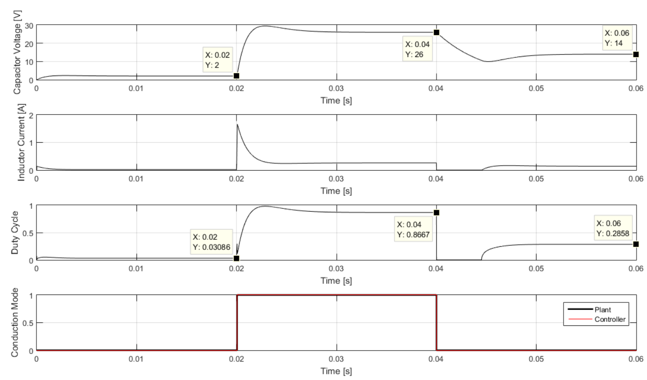

Fig. 12. Buck simulation output with same parameters.

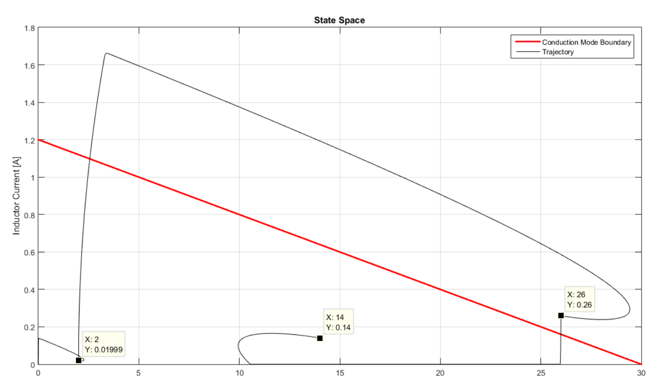

Fig. 13. Buck simulation output with same parameters in state space.

V. Conclusions

The modeling and control of the buck converter in mixed conduction mode is far from trivial. Even considering it ideal,

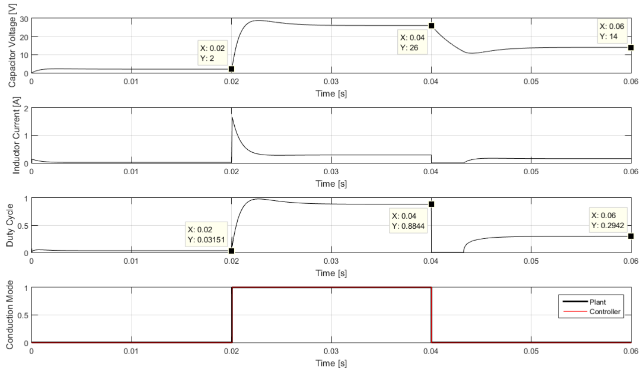

Fig. 14. Buck simulation output with decreased parameters.

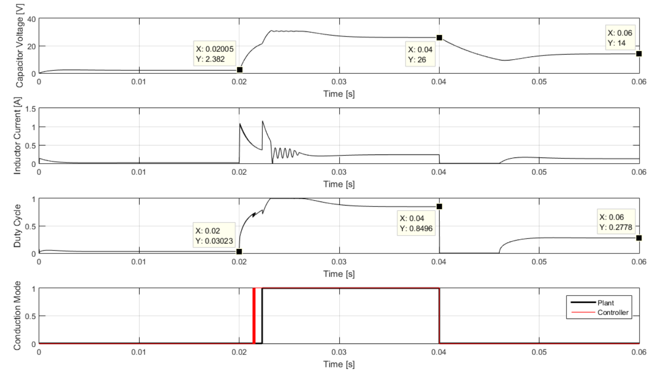

Fig. 16. Buck simulation output with increased parameters.

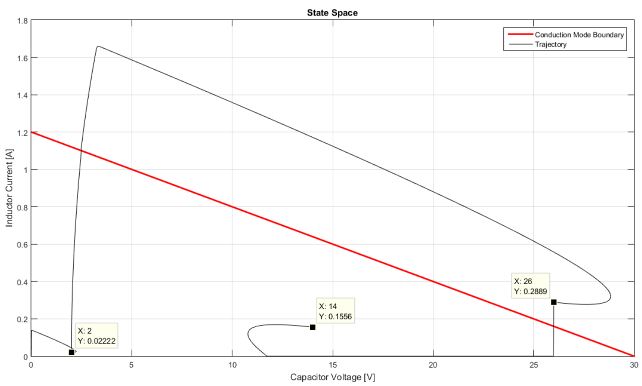

Fig. 15. Buck simulation output with decreased parameters in state space.

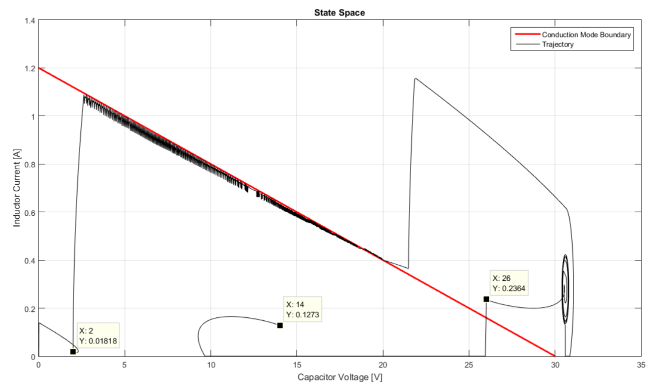

Fig. 17. Buck simulation output with increased parameters in state space.

it's strongly nonlinear, because its non-smooth vector field (1). Unfortunately, this characteristic doesn't vanish on the SSA models: (4) for CCM, (12) for DCM and (16) for the BCM criteria.

The input-output linearizations (22) for DCM and (44) for CCM are necessary for the design of both pole placement and sliding-mode, but the parameter mismatch can only be treated with the last one. And, without parameter identification [11], the steady error can only be zeroed with a sliding-mode integral action approach, which is very successful as shown in figures 12, 14 and 16.

References

[1] Sira-Ramírez, H. and R. Silva-Ortigoza. "Control Design Techniques in Power Electronics Devices." (2006).
[2] Erickson and R. Maksimović. "Fundamentals of Power Electronics, 3rd edition." (2020).
[3] Jian Sun, D. M. Mitchell, M. F. Greuel, P. T. Krein and R. M. Bass, "Averaged modeling of PWM converters operating in discontinuous conduction mode," in IEEE Transactions on Power Electronics, vol. 16, no. 4, pp. 482-492, July 2001, doi: 10.1109/63.931052.
[4] Kazimierczuk, M.. "Pulse-Width Modulated DC-DC Power Converters, 2nd edition." (2016).
[5] Slotine, J. and Weiping Li. "Applied Nonlinear Control." (1991).
[6] Isidori, A.. "Nonlinear Control Systems, Third Edition." Communications and Control Engineering (1995).
[7] Sastry, S.. "Nonlinear Systems: Analysis, Stability, and Control." (1999).
[8] M. Guay and P. J. McLellan, "Input-output linearization of general nonlinear control systems," Proceedings of 1994 American Control Conference - ACC '94, 1994, pp. 2695-2699 vol.3, doi: 10.1109/ACC.1994.735051.
[9] Friedland, B. and W. Stephen. "Control System Design: An Introduction to State-Space Methods." (1987).
[10] Zeitz, M. "The extended Luenberger observer for nonlinear systems." Systems & Control Letters 9 (1987): 149-156.
[11] Shtessel, Y. et al. "Sliding Mode Control and Observation." (2013).